Journal of Applied Mechanics and Technical Physics, Vol. 43, No. 6, pp. 847–853, 2002

CALCULATION OF THE DIFFERENTIAL ROTATION OF A RIGID CORE IN HYPOPLASTIC MEDIA UNDER COMPLEX LOADING

S. V. Lavrikov

UDC 539.37

The plane problem of calculating the directional transfer of internal masses and the differential rotation of an internal rigid core is considered for hypoplastic media with continuous rotation of the principal axes of the strain tensor under complex loading. The hypoplastic model of granular media with internal variables is used as the basic model. A numerical algorithm for calculating stress and velocity fields in an inelastic medium under complex loading is developed using the finite-element method. Mechanical trajectories of material points of the medium are calculated and the rotational velocity of the core and the reduction coefficient are estimated.

Introduction. Directional mass transfer in inelastic media under complex loading was revealed experimentally in [1–7]. Revuzhenko and Bobryakov [1, 2] experimentally modeled the homogeneous loading of a loose medium involving the rotation of the principal axes of the strain tensor. The medium was loaded in the following manner. Initially, the inelastic body was simultaneously subjected to tension and compression in orthogonal directions. A Cartesian coordinate system with two axes coinciding with the compression and tension directions was introduced. Then, the tension and compression directions were rotated through an angle α around the third coordinate axis. Given the continuous dependence of the angle α on time, the loading process described above was a complex loading with continuous rotation of the strain-tensor principal axes. Obviously, if a body is extended and compressed in mutually orthogonal directions in a certain coordinate system, there always exists a coordinate system in which this loading is pure shear. Therefore, the loading described above can be interpreted as shear whose direction varies continuously.

In [1–7], it was shown that to ensure the loading conditions described above in experiment, one needs to use a material specimen shaped like an elliptic cylinder with the x_3 axis and specify the velocity vector $\boldsymbol{v}_1$ on the lateral elliptic surface in the x_1x_2 plane which satisfies the Kepler condition

$$\boldsymbol{v}_1 \cdot \boldsymbol{n}_1 = 0, \qquad |\boldsymbol{v}_1 \times \boldsymbol{r}| = \text{const}, \tag{1}$$

where $\boldsymbol{n}_1$ is the normal vector to the lateral surface of the specimen and $\boldsymbol{r}$ is the radius vector (Fig. 1). In this case, the stress–strain state in the elliptic cylinder is spatially homogeneous, irrespective of the rheological properties of the medium [8] (it is only required that the medium be rheologically stable, i.e., localization, fracture, etc., be absent). However, both conditions (1) are rather difficult to realize in practice. Therefore, in the laboratory experiments in [1–7], only the main features of the ideal situation were preserved — the first condition in (1) was satisfied, whereas the second condition was replaced by the condition of constant velocity:

$$\boldsymbol{v}_1 \cdot \boldsymbol{n}_1 = 0, \qquad |\boldsymbol{v}_1| = \text{const}. \tag{2}$$

It is clear that replacement of (1) by (2) leads to some inhomogeneity, which is the smaller the closer the ellipse to a circle (Fig. 1). In other words, for small eccentricity of the ellipse, loadings under conditions (1) and (2) lead to close results. It was found, however, that weak inhomogeneity introduced into the loading conditions leads to the following effect. In one complete revolution of the tension and compression directions around the body (one loading cycle), all its internal material points describe almost closed trajectories but do not return to their initial

Mining Institute, Siberian Division, Russian Academy of Sciences, Novosibirsk 630091. Translated from Prikladnaya Mekhanika i Tekhnicheskaya Fizika, Vol. 43, No. 6, pp. 75–83, November–December, 2002. Original article submitted November 22, 2001; revision submitted January 17, 2002.

0021-8944/02/4306-0847 $27.00

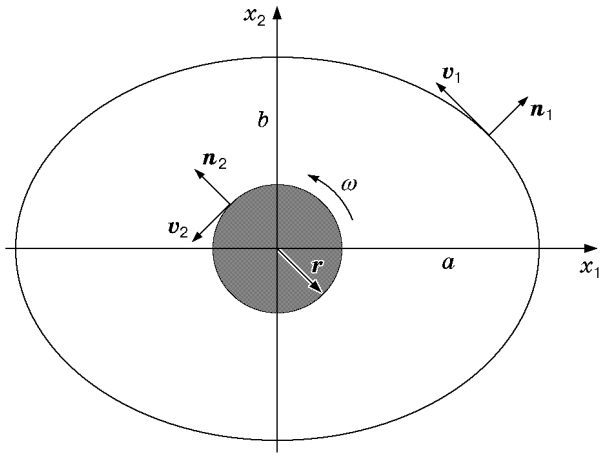

Fig. 1

Fig. 2

positions (as would be the case if the deformation were strictly homogeneous). As the number of loading cycles increases, the initial, closely spaced points move farther and farther apart.

Figure 2, borrowed from [1], shows experimental results for a loose material after several loading cycles. Before deformation, the points located along the major axis of the ellipse were painted black. A special feature of the process described above is that the internal deformation is potentially unlimited if the external volume of body remains unchanged.

It was also shown experimentally [7] that if a rigid core is placed in a body, it is set in motion during deformation and begins to rotate. It is worth noting that the direction of rotation of the core depends on the medium's rheology. For example, for a viscous liquid, the core always rotates in the loading direction (rotation of the tension and compression directions). The core in a loose medium can rotate both in the loading direction and in the opposite direction, depending on the loading conditions.

Based on the effect revealed, Revuzhenko et al. [1–7] proposed a possible mechanism for the directional transfer of the internal masses of the Earth and differential rotation of its solid core due to the diurnal rotation of the planet in the tidal-force fields of the Moon or the Sun.

The goal of this paper is numerical modeling of the deformation process described above and calculation of the directional mass transfer and differential rotation of a rigid core in an inelastic medium under complex loading. However, the possibility of using calculation results to estimate the directional transfer of the internal masses of the Earth and differential rotation of its solid core calls for additional analysis and is not considered here.

To solve most of the applied problems of mechanics, it is necessary to construct a mathematical model of a medium that adequately describe the effects occurring during deformation. For our purposes, we need a mathematical model that describes, first, the inelastic response of a medium, second, complex loading for which the strain-tensor principal axes rotate continuously, and third, the possible unloading of the material during deformation and repeated loading, i.e., cyclic loading. Among these models are so-called hypoplastic models [9, 10], characterized by strongly nonlinear equations even for increments, which makes it possible to describe both active loading and unloading of an inelastic medium using the same equations. We dwell on the hypoplastic model of loose media [11]. It was previously verified for various loading paths including complex paths. Kolymbas et al. [12, 13] showed that this model satisfactorily describes dilatancy and stresses in loose media. Moreover, the model adequately describes the response of the medium to cyclic loading, including intermediate unloading. However, in [13] it was noted that the hypoplastic model of [11] fails to describe the alignment condition for complex loading of loose media. As laboratory experiments [1, 2] showed, for a loose medium under complex loading with continuous rotation of the strain-tensor principal axes, the alignment condition holds for the stress and strain tensors, whereas the hypoplastic

model of [11] approximately satisfies the alignment condition for stress and strain-rate tensors, which holds for viscous liquids. Since the experimentally detected effect of directional mass transfer and core differential rotation is observed for both loose and viscous media, we confine our attention to the hypoplastic model [11].

Formulation of the Problem. We consider the problem of mass transfer and core differential rotation for complex loading. As mentioned above, the effect of directional transfer is observed in the plane of rotation of the strain-tensor principal axes. In this case, it makes sense to treat the problem in a plane formulation. According to [11], the governing equations of the hypoplastic model for loose media with internal variables, which relate the stress tensor T to the strain-rate tensor D, are written in general form

$$\overset{\circ}{T} = C_1 \operatorname{tr}(T+S) + C_2 \frac{\operatorname{tr}((T+S)D)}{\operatorname{tr}(T+S)}(T+S) + \Big[\frac{C_3 T^2 + C_4 T^{*^2}}{\operatorname{tr} T} + \frac{C_5 T^3 + C_6 T^{*^3}}{\operatorname{tr} T^2}\Big]\sqrt{\operatorname{tr} D^2},$$

$$\dot{e} = (1+e)\operatorname{tr} D; \tag{3}$$

$$S = sE, \quad p = \operatorname{tr} T, \quad \overset{\circ}{T} = \dot{T} - WT + TW, \quad T^* = T - pE/3, \quad W = (\nabla \boldsymbol{v} - \nabla \boldsymbol{v}^{\mathrm{t}})/2, \tag{4}$$

$$s = [s_0 + k(p/p_0)^{\beta} \ln((1+e)/(1+e_0))](p/p_0)^{\alpha}, \quad k = -s_0/[(p_r/p_0)^{\beta} \ln((1+e_r)/(1+e_0))],$$

where $\boldsymbol{v}$ is the velocity field, E is the unit tensor, and e is the porosity. The model constants are as follows:

$$C_1 = -103.01, \quad C_2 = -197.61, \quad C_3 = 37.24,$$

$$C_4 = 1572.92, \quad C_5 = -394.69, \quad C_6 = -1265.66,$$

$$p_r = -0.5 \text{ MPa}, \quad p_0 = 0.729 \text{ MPa}, \quad s_0 = -0.149 \text{ MPa}, \tag{5}$$

$$\alpha = 0.6, \quad \beta = 0.1, \quad e_r = 0.73, \quad e_0 = 0.54.$$

Relations (3)–(5) are written for the three-dimensional case. Reducing Eqs. (3)–(5) to the case of plane stresses, we obtain a system of equations for increments of the stress-tensor components $\Delta\sigma_{11}$, $\Delta\sigma_{22}$, and $\Delta\sigma_{12}$ and displacement-field components Δu_1 and Δu_2 in closed form:

$$\frac{\partial \Delta\sigma_{11}}{\partial x_1} + \frac{\partial \Delta\sigma_{12}}{\partial x_2} = 0, \qquad \frac{\partial \Delta\sigma_{12}}{\partial x_1} + \frac{\partial \Delta\sigma_{22}}{\partial x_2} = 0; \tag{6}$$

$$\begin{aligned}
\Delta\sigma_{11} &= A_{11}\frac{\partial \Delta u_1}{\partial x_1} + A_{12}\frac{\partial \Delta u_1}{\partial x_2} + A_{13}\frac{\partial \Delta u_2}{\partial x_1} + A_{14}\frac{\partial \Delta u_2}{\partial x_2} + A_{15}\frac{\partial \Delta u_3}{\partial x_3} + A_{16}\Delta L,\\
\Delta\sigma_{22} &= A_{21}\frac{\partial \Delta u_1}{\partial x_1} + A_{22}\frac{\partial \Delta u_1}{\partial x_2} + A_{23}\frac{\partial \Delta u_2}{\partial x_1} + A_{24}\frac{\partial \Delta u_2}{\partial x_2} + A_{25}\frac{\partial \Delta u_3}{\partial x_3} + A_{26}\Delta L,\\
\Delta\sigma_{12} &= A_{31}\frac{\partial \Delta u_1}{\partial x_1} + A_{32}\frac{\partial \Delta u_1}{\partial x_2} + A_{33}\frac{\partial \Delta u_2}{\partial x_1} + A_{34}\frac{\partial \Delta u_2}{\partial x_2} + A_{35}\frac{\partial \Delta u_3}{\partial x_3} + A_{36}\,\Delta L,\\
\Delta\sigma_{33} &= A_{41}\frac{\partial \Delta u_1}{\partial x_1} + A_{42}\frac{\partial \Delta u_1}{\partial x_2} + A_{43}\frac{\partial \Delta u_2}{\partial x_1} + A_{44}\frac{\partial \Delta u_2}{\partial x_2} + A_{45}\frac{\partial \Delta u_3}{\partial x_3} + A_{46}\Delta L = 0,
\end{aligned} \tag{7}$$

$$\Delta L = \sqrt{\Big(\frac{\partial \Delta u_1}{\partial x_1}\Big)^2 + \frac{1}{2}\Big(\frac{\partial \Delta u_2}{\partial x_1} + \frac{\partial \Delta u_1}{\partial x_2}\Big)^2 + \Big(\frac{\partial \Delta u_2}{\partial x_2}\Big)^2 + \Big(\frac{\partial \Delta u_3}{\partial x_3}\Big)^2},$$

$$\Delta e = (1+e)\Big(\frac{\partial \Delta u_1}{\partial x_1} + \frac{\partial \Delta u_2}{\partial x_2} + \frac{\partial \Delta u_3}{\partial x_3}\Big).$$

Equations (6) are the equations of equilibrium for increments of the plane-stress tensor components. Equations (7) are the constitutive relations of the hypoplastic model, where the quantities A_{ij} ($i = \overline{1,4}$ and $j = \overline{1,6}$) depend only on the stresses σ_{ij}, porosity e, and model constants and do not depend on the increments of stresses and porosity. In (7), the nonlinear part of the equations of the model is denoted by ΔL. The equation $\Delta\sigma_{33} = 0$ is the assumption for plane stresses and serves to eliminate the quantity $\partial\Delta u_3/\partial$, which describes the volume change due to deformation (dilatancy), from Eqs. (7).

Equations (6) and (7) are subjected to the boundary conditions

$$\Delta \boldsymbol{u}_1 \cdot \boldsymbol{n}_1 = 0, \qquad |\Delta \boldsymbol{u}_1| = d = \text{const}; \tag{8}$$

$$\Delta \boldsymbol{u}_2 \cdot \boldsymbol{n}_2 = 0, \qquad \omega = \text{const}. \tag{9}$$

Conditions (8) refer to the external boundary of the elliptic region (see Fig. 1) and, according to [1–7], they ensure the directional transfer effect. In solving the problem numerically, we use the quantity d in (8) as a loading parameter. Conditions (9) refer to the boundary of the nonfixed rigid core placed at the center of the region. The angular velocity of the core, denoted by ω in (9), is assumed to be an unknown constant and is determined from the additional condition that the total rotational moment vanishes at the core boundary:

$$M = 0. \tag{10}$$

In other words, if the rotational moment occurs at the core boundary during deformation, it is compensated for by rotation of the core. Conditions (9) and (10) allow us to calculate the direction and angular rotation of the core and, hence, the reduction coefficient (ratio of the number of revolutions of the core to the number of loading cycles).

Thus, system (6), (7) subject to boundary conditions (8)–(10) is a closed model for calculating the increments of stress $\Delta\sigma_{ij}$, displacements Δu_i, and porosity Δe.

We solve problem (6)–(10) numerically using the finite-element method (FEM). The standard technique of solving boundary-value problems by the FEM reduces the original system of differential equations to a high-order algebraic system [14, 15]. Since the governing equations (7) are nonlinear, the use of the FEM leads to a nonlinear system of algebraic equations of the form

$$F_1(y_1, \ldots, y_m) = 0, \quad \ldots, \quad F_m(y_1, \ldots, y_m) = 0. \tag{11}$$

Here the components of the vector $\boldsymbol{y} = (y_1, \ldots, y_m)$ are the increments of the displacements Δu_1 and Δu_2 at the nodes of the finite-element mesh. The nonlinear system (11) is solved by the Newton iterative method

$$\boldsymbol{y}^{k+1} = \boldsymbol{y}^k - J^{-1}(\boldsymbol{y}^k)\boldsymbol{F}(\boldsymbol{y}^k), \tag{12}$$

where the superscript k denotes the iteration number and J is a Jacobi matrix:

$$J = \begin{pmatrix} \partial F_1/\partial y_1 & \ldots & \partial F_1/\partial y_m \\ \ldots\ldots\ldots\ldots\ldots\ldots\ldots & & \\ \partial F_m/\partial y_1 & \ldots & \partial F_m/\partial y_m \end{pmatrix}.$$

As the convergence criterion of the iterative process (12), we use the condition $\max\limits_{1 \leqslant i \leqslant m} |F_i(\boldsymbol{y}^k)| < \varepsilon$ (ε is a known small quantity). In this manner, one loading step is performed. Since the equations of the model are nonlinear in increments, we construct a complete solution of the problem using the iterative scheme

$$\sigma_{ij}^{n+1} = \sigma_{ij}^n + \Delta\sigma_{ij}^n, \quad u_i^{n+1} = u_i^n + \Delta u_i^n, \quad e^{n+1} = e^n + \Delta e^n \quad (i, j = 1, 2), \tag{13}$$

where the increments at the nth loading step are determined by solving the boundary-value problem (6)–(10).

For numerical implementation of the iterative process (13), it is necessary to determine the initial stresses of the medium. It was found experimentally [1–7] that whatever the state of the medium at the initial moment, the deformation process is stabilized after a time, i.e., it reaches a steady regime. For this regime, all stresses remain unchanged with time. The properties of loose materials are such that the medium adapts itself to the deformation conditions and "forgets" the loading history. In other words, the steady stresses depend only on the current loading conditions and do not depend on the initial stresses. Thus, the iterative process (13) should be performed until the deformation process becomes steady. As the criterion of steady deformation, we use the condition $\max\limits_{i,j} |\Delta\tilde{\sigma}_{ij}^n/\tilde{d}| \ll 1$, where $\Delta\tilde{\sigma}_{ij}^n$ is the increment of dimensionless stresses at the nth iteration of the process (13) and $\tilde{d}$ is the dimensionless loading parameter from boundary condition (8). In other words, it is assumed that the deformation becomes steady if the calculated stress increments are close to zero regardless of the order of smallness of the loading parameter.

A preliminary analysis of the adopted hypoplastic model performed for homogeneous deformation shows that the model adequately describes stabilization and attainment of a steady deformation regime [12, 13]. For homogeneous deformation [with conditions (1) at the external boundary], the steady state is easily determined; at

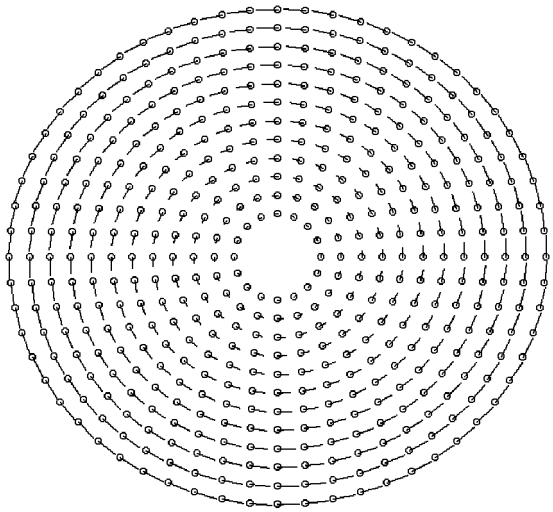

Fig. 3

least, one need not solve the boundary-value problem. At the same time, as noted above, loading conditions of the type (1) and (2) for small eccentricities of the ellipse give close results. Therefore, if the stress state reached for steady homogeneous deformation under condition (1) at the external boundary is used as the initial state for problem (8)-(10), one might expect that the resulting solution for the increments $\Delta\sigma_{ij}$ tends to zero, which corresponds to a steady deformation regime. The experience of using hypoplastic models to solve plane boundary-value problems shows that even after the first iteration of the process (13), this technique gives a solution that describes the steady state with reasonable accuracy [16].

Calculation Results. We consider the following example. The parameters of the calculation region and the initial stress state of a medium are as follows:

$$a/b = 1.1, \quad r/b = 0.21, \quad e = 0.837\,11, \quad \varepsilon = 10^{-9},$$
$$\sigma_{33} = -20 \text{ KPa}, \quad \sigma_{11} = 1.25\sigma_{33}, \quad \sigma_{22} = 1.19\sigma_{33}, \quad \sigma_{12} = 0.7\sigma_{33}. \tag{14}$$

Here a and b are the major and minor semiaxes of the ellipse, respectively, and r is the radius of the internal core (see Fig. 1). The stress state (14) is obtained as a homogeneous steady state of the medium using the hypoplastic model (3)–(5) [12, 13].

Numerical solution of problem (6), (7) subject to the boundary conditions (8)–(10) shows that even after the first iteration, the resulting increments of the stress-tensor components are equal to zero with an accuracy of 7%, i.e., $\max\limits_{i,j} |\Delta\tilde{\sigma}^n_{ij}/\tilde{d}| = 0.07$. As expected, one iteration suffices to obtain the steady state with reasonable accuracy. Thus, the increment of the displacement field $\Delta\boldsymbol{u}$ (Fig. 3) obtained after the first iteration can be interpreted as a steady velocity field that occurs in a loose medium under complex loading with continuous rotation of the strain-tensor principal axes.

The field $\Delta\boldsymbol{u}$ was integrated numerically by the standard Euler method, and trajectories of material points of the medium were determined. Calculations show that the trajectories are closed elliptic curves. However, the periods of revolution of different points along these trajectories are different. We consider the points lying on the major semiaxis of the ellipse before deformation. Calculations show that all the internal points do not return to the initial positions in one deformation cycle (one complete revolution of a material point on the external boundary of the ellipse) and occupy new positions. The new and initial positions differ insignificantly from each other by virtue of small eccentricity of the ellipse. Nonetheless, this difference becomes more pronounced as the number of cycles increases. Figure 4a shows trajectories and final positions of the observed material points after the first three loading cycles. One can see that the initial line passing through the points of the major axis becomes a curve. Figure 4b shows the deformation stage corresponding to 15 complete loading cycles. An analysis of the calculation results shows that the directional transfer of internal masses occurs in the medium under complex loading with continuous rotation of the strain-tensor principal axes.

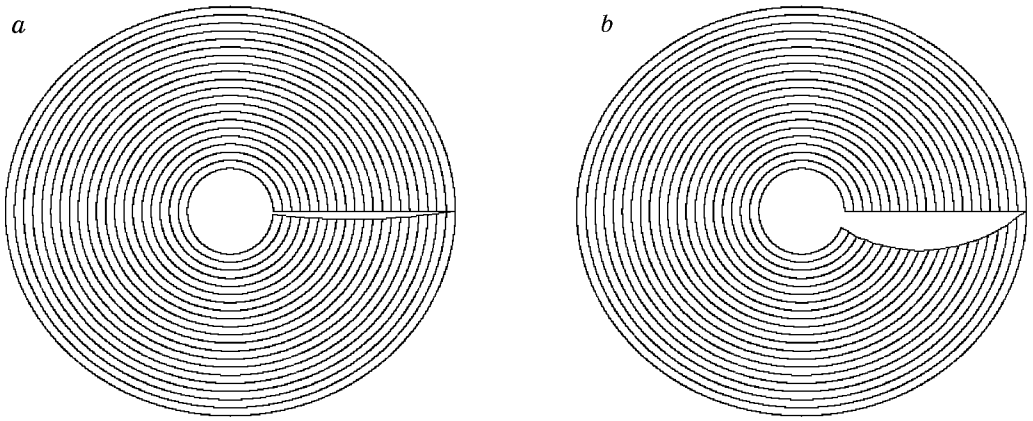

Fig. 4

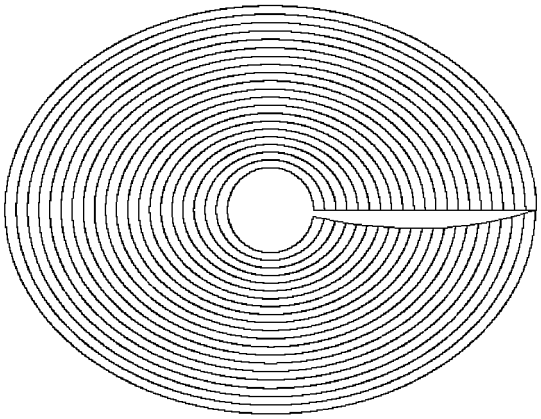

Fig. 5

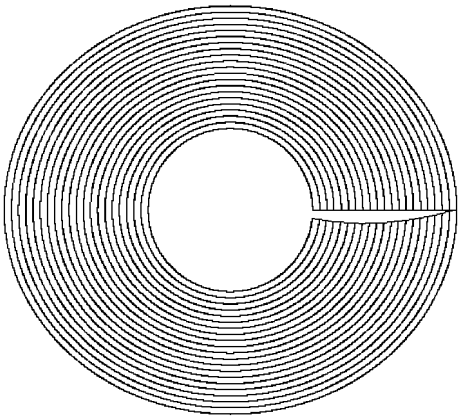

Fig. 6

From the calculation results (Fig. 4) it also follows that the internal rigid core begins to rotate during deformation. In each loading cycle, the core rotates through an angle somewhat smaller than 2π, i.e., it rotates in the loading direction but lags behind in rotational velocity. As the number of loading cycles increases, this lag becomes more pronounced (Fig. 4). This result comes as no surprise. As follows from the experiments in [1–7], the internal core can rotate in the loading direction (loading of viscous liquids) and in the opposite direction (loading of loose media). As a whole, the hypoplastic model (3)–(5) adequately describes the behavior of loose media. At the same time, calculations using this model show that the alignment condition holds approximately for the stress and strain-rate tensors, which is the case for viscous liquids. Apparently, the direction of rotation of the internal core depends on whether or not the alignment condition holds. For the chosen parameters of the calculation region (14), the core rotates through an angle which is 1.48° smaller than 2π. Thus, the reduction coefficient is equal to 0.9958.

The results obtained depend strongly on the geometrical parameters of the calculation region. Calculations were performed for various values of a/b and r/b. Thus, as the ratio a/b (eccentricity of the ellipse) increases, the effect of directional mass transfer and differential rotation of the core becomes more pronounced for a smaller number of loading cycles. For example, for $a/b = 1.3$, initially close points move far apart even after one loading cycle. In this case, the core rotates through an angle that differs from an angle of 2π by 9.13° and the reduction coefficient decreases to 0.9746 (Fig. 5). The reverse situation is observed if the ratio r/b in (14) increases, i.e., the size of the internal core increases. For example, for $r/b = 0.4$, the directional transfer effect is less pronounced compared to the case of parameters (14). Figure 6 shows trajectories of material points after six loading cycles. In this case, after one loading cycle, the internal core rotates through an angle that differs from an angle of 2π by 1.02°, and hence, the reduction coefficient is equal to 0.9972.

Conclusions. The calculation results lead to the following conclusions. Hypoplastic models with internal variables satisfactorily describe the behavior of loose materials and can be used to solve boundary-value problems.

Complex loading of inelastic media with continuous rotation of the strain-tensor principal axes leads to stable directional transfer of internal masses of the medium. In this case, the internal deformation is accumulated with time and is potentially unlimited.

During loading, a nonfixed rigid core in a material specimen is set in motion and begins to rotate. Rotation of the core calculated using the hypoplastic model agrees qualitatively with experimental data on loading of viscous liquids. Angular velocities of the core and reduction coefficients are estimated for various geometrical parameters of the calculation region.

The author is grateful to D. Kolymbas and A. F. Revuzhenko for useful discussions of the work.

The work was supported by the INTAS International Foundation (Grant Nos. 95-0742 and YSF 98-178).

REFERENCES

1. A. F. Revuzhenko, *Mechanics of Elastoplastic Media and Nonstandard Analysis* [in Russian], Izd. Novosib. Univ., Novosibirsk (2000).
2. A. P. Bobryakov and A. F. Revuzhenko, "A method for testing inelastic materials," *Izv. Akad. Nauk SSSR, Mekh. Tverd. Tela*, No. 4, 178–182 (1990).
3. A. P. Bobryakov, A. F. Revuzhenko, and E. I. Shemyakin, "Possible mechanism of the Earth's mass transfer," *Dokl. Akad. Nauk SSSR*, **272**, No. 5, 1097–1099 (1983).
4. A. F. Revuzhenko, "Tidal mechanism of mass transfer," *Izv. Akad. Nauk SSSR, Fiz. Zemli*, No. 6, 13–20 (1991).
5. A. P. Bobryakov, A. F. Revuzhenko, and E. I. Shemyakin, "Tidal deformation of planets: Experimental modeling," *Geotektonika*, No. 6, 21–34 (1991).
6. A. F. Revuzhenko, "A class of composite loads for an inelastic material," *J. Appl. Mech. Tech. Phys.*, No. 5, 772–778 (1986).
7. A. F. Revuzhenko, V. P. Kosykh, and A. P. Bobryakov, "Localized plastic flow of a geomedium around a rigid inclusion," *Fiz. Tekh. Probl. Razrab. Polezn. Iskop.*, No. 6, 27–34 (1998).
8. A. F. Revuzhenko, "The simplest flows of a continuum," *Dokl. Akad. Nauk SSSR*, **303**, No. 1, 54–58 (1988).
9. D. Kolymbas and W. Wu, "Introduction to hypoplasticity," in: D. Kolymbas (ed.), *Modern Approaches to Plasticity*, Elsevier, Amsterdam (1993), pp. 213–223.
10. D. Kolymbas, "Computer-aided design of constitutive laws," *Int. J. Num. Anal. Meth. Geomech.*, **15**, 593–604 (1991).
11. D. Kolymbas, I. Herle, and P.-A. von Wolffersdorff, "Hypoplastic constitutive equation with internal variables," *Int. J. Num. Anal. Meth. Geomech.*, **19**, 415–436 (1995).
12. D. Kolymbas, S. V. Lavrikov, and A. F. Revuzhenko, "Homogeneous deformation of a loose medium. Theory and experiment," *Prikl. Mekh. Tekh. Fiz.*, **35**, No. 6, 114–121 (1994).
13. D. Kolymbas, S. V. Lavrikov, and A. F. Revuzhenko, "Method of analysis of mathematical models of media under complex loading," *J. Appl. Mech. Tech. Phys.*, **40**, No. 5, 895–902 (1999).
14. O. Z. Zienkiewicz, *The Finite Element Method*, McGraw–Hill, London (1977).
15. K.-J. Bathe and E. L. Wilson, *Numerical Methods in Finite Element Analysis*, Prentice-Hall, Englewood Cliffs, New Jersey (1976).
16. S. V. Lavrikov and A. F. Revuzhenko, "Complex loading of heterogeneous materials with redistribution of internal mass," *J. Theor. Appl. Fract. Mech.*, **29**, 85–91 (1998).